Polymer networks between two parallel planar surfaces

2003 J. Phys. A: Math. Gen. 36 8249

(http://iopscience.iop.org/0305-4470/36/30/304)

INSTITUTE OF PHYSICS PUBLISHING JOURNAL OF PHYSICS A: MATHEMATICAL AND GENERAL

J. Phys. A: Math. Gen. **36** (2003) 8249–8264 PII: S0305-4470(03)61053-X

Polymer networks between two parallel planar surfaces

W L Vandoolaeghe and K K Müller-Nedebock

Department of Physics, University of Stellenbosch, Private Bag X1, 7602 Matieland, South Africa

E-mail: wlv@physics.sun.ac.za and kkmn@physics.sun.ac.za

Received 18 March 2003, in final form 10 June 2003
Published 16 July 2003
Online at stacks.iop.org/JPhysA/36/8249

Abstract

The formation and mechanical properties of a polymer network on and between two flat parallel surfaces are investigated. Most treatments of surface-attached polymers have been limited to scaling theory. In the present investigation we probe the physics of the system by means of a mathematical description of the *random* crosslinking of ideal (or *phantom*) chains. We modify an existing *bulk* model of network formation by Deam and Edwards, with polymer–polymer crosslinks, to include surfaces and polymer–surface crosslinks. We investigate two variations of this model: in the first place, the polymer–surface links are formed anywhere along the contours of the long, ideal polymer chains. In the second *brush* network model, the surface links are restricted to one endpoint of each macromolecule. Within the framework of replica theory, we compute statistical averages and the elastic properties of the systems such as the stress–strain relationship. In both cases the elastic modulus of the bulk network is altered, and has a characteristic form due to the confinement. Furthermore, we find that the stress–strain relationship depends on the *manner* of crosslinking.

PACS numbers: 61.41.+e, 82.35.Gh

1. Introduction

Polymers in confining geometries exhibit very specific and interesting properties. In particular, understanding the formation and properties of polymer *networks* crosslinked at and between surfaces is crucial for a number of applications, where surfaces have to be protected against forms of mechanical or chemical stress, such as abrasion and corrosion [1]. Surface-attached networks also play an important role in several biomedical concepts, for example, to provide biocompatible, but stable coatings on implant surfaces [2]. Most theoretical treatments of these types of systems have been on the level of scaling theory [3], with few analytical approaches. Recently, Allegra and Raos [4] investigated a confined polymer network, without

the possibility of wall attachments, and modelled the effect of confining walls by a harmonic potential.

In this work, we investigate the elastic properties of a polymer network that has formed between two, parallel planar surfaces. The spacing h_z between the walls is chosen to be narrow relative to the average size of the polymer. We model the system as a three-dimensional network of long macromolecules that form permanent, but random, bonds with each other as well as with the confining surfaces. The chains are assumed to be ideal. Consequently, the calculations presented here will only involve the bulk crosslinks, surface attachments and confinement of Gaussian chains, neglecting both internal energy contributions and topology (entanglement constraints). The ideal or *phantom* model is the customary first approach in solving polymer theory problems.

In this paper, we focus on evaluating the free energy of deformation to determine the stress–strain relationship for the securely gelled network system. As a rule, a gel sample's volume will be conserved during strain. The *macroscopic* deformation of a point, $\mathbf{r} \to \mathbf{r}' = \mathbf{\Lambda} \cdot \mathbf{r}$, where

$$\mathbf{\Lambda} = \begin{pmatrix} \lambda^{-\frac{1}{2}} & 0 & 0 \\ 0 & \lambda^{-\frac{1}{2}} & 0 \\ 0 & 0 & \lambda \end{pmatrix} \qquad \lambda > 0 \tag{1.1}$$

is then suitably described by the above isovolumetric deformation tensor $\mathbf{\Lambda}$ [5]. The constancy of volume during deformation makes it possible to define the complete state of strain in terms of a single parameter λ. In the simplest, ideal case, the crosslinks together with entropic spring behaviour of the chains are responsible for network elasticity. The classical theory of rubber elasticity [6] predicts that the free energy $\mathcal{F}$ of deformation is proportional to the sum of squares of the principle extension ratios:

$$\mathcal{F} = N_{\mathrm{c}} k_{\mathrm{B}} T \sum_{i=x,y,z} \lambda_i^2 \tag{1.2}$$

where k_{B} is the Boltzmann constant, T is the temperature and N_{c} is the crosslink density of the network sample. A major discrepancy of this model is that it assumes an *affine* deformation: if a macroscopic network sample is deformed by $\mathbf{\Lambda}$, then the end-to-end vector $\mathbf{R}$ of any subchain between two junction points will be equal to $\mathbf{\Lambda} \cdot \mathbf{R}$, after deformation. The affinity assumption implies that the crosslinks do not fluctuate around their affinely deformed positions. In the James and Guth model [7], the crosslinks are essentially unrestricted, and the resultant free energy in (1.2) is altered by a factor of $\frac{1}{2}$.

In 1975 a pioneering network model was introduced by Deam and Edwards [8], which models the effect of the network on a given chain by a harmonic localizing potential. In order to calculate the free energy of deformation, they resorted to a variational approach and the replica method familiar from spin glass theory [9]. The resultant Deam and Edwards free energy (for a network regarded as one giant chain of contour length $\mathcal{L}$, cut-off length ℓ_{c} and effective segment ℓ—also known as the Kuhn length—such that $L \gg \ell$ for a flexible chain)

$$\mathcal{F}_{\mathrm{DE}} \leqslant k_{\mathrm{B}} T \left[\frac{1}{2} \frac{N_{\mathrm{c}}}{(1 + c/\rho)} \sum_{i=x,y,z} \lambda_i^2 - \frac{3N_{\mathrm{c}}}{2} \ln \frac{6N_{\mathrm{c}}}{\ell L} + \frac{3N_{\mathrm{c}}}{2} \right] \tag{1.3}$$

with constants given by

$$c \equiv \frac{1}{2\sqrt{\ell_{\mathrm{c}}}} \left(\frac{3}{2\pi \ell} \right)^{\frac{3}{2}} \quad \text{and} \quad \rho \equiv \mathcal{L}/V \tag{1.4}$$

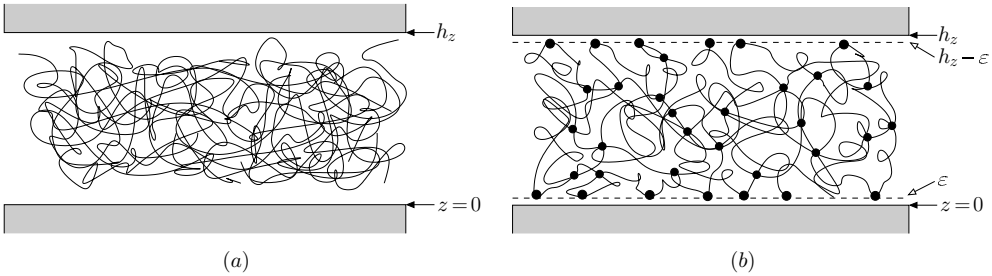

Figure 1. (*a*) A simplified illustration of a very dense melt of ideal chains, confined between two walls. (*b*) A confined surface-attached network. The wall links are situated an infinitesimal distance ε from the wall surface.

again shows the same strain dependence as (1.2), but with a different front factor and more terms depending on the crosslink density, not the affine deformation.

A more recent network model by Panyukov and Rabin [10], based on the Deam and Edwards model of instantaneous crosslinking of ideal chains, confirms the free energy (1.3). However, they obtain a mean-field free energy by means of an elegant field theoretic method involving a double limiting procedure: the replica trick *and* a generalization of the deGennes' $n = 0$ method. In this paper, the aim is to use the Deam and Edwards concept of a harmonic localizing potential variational ansatz as a more intuitive approach to treating the crosslink constraints. We start by expressing the partition function of the system. This is done by adapting the Deam and Edwards [8] model of bulk network formation so that it incorporates the surface restrictions as well as additional surface–polymer crosslinks as mathematical constraints in the partition function.

A great number of chemical fabrication techniques will give rise to such a surface-attached network [11, 12]. We therefore explore two statistical mechanics models, both rooted in the Deam and Edwards theory, but corresponding to different preparation routes. In the first case, both crosslinks of the network and surface bonds are formed simultaneously from a collection of confined chains. The effect of the crosslinked network on a given chain segment (monomer) is modelled by placing each monomer in a *homogeneous* harmonic localizing potential. In the second model, the network crosslinking takes place in a *brush*-like system of surface-attached polymer chains. In this case, we impose an *inhomogeneous* harmonic localizing potential. Both models accommodate instantaneous crosslinking, which facilitates computation within the framework of equilibrium statistical mechanics.

The paper is organized as follows: first we present the homogeneous localization formalism (melt network model), variational calculation and results. A similar treatment for the *inhomogeneous* localization case (brush network model) follows in section 3. We compare the results of the two models and summarize our findings in the concluding section.

2. The melt network

Let a single long flexible macromolecule of total contourlength L be denoted by the path $\mathbf{R}(s)$, where $s \in [0, L]$ is the arclength coordinate. Prior to linking, we have a melt comprising M independent ideal chains, which may be visualized as a rather dense, overlapping and interpenetrating polymer solution. All forces between the chains, except at points of crosslinkage, are ignored and each chain is assumed to be free to take on any conformation in the confined region. The confinement formalism must ensure that all the chains vanish beyond the boundaries, situated at say $z = 0$ and $z = h_z$, as illustrated in figure 1(*a*).

We assign to each macromolecule a statistical weight given by the Wiener measure [13]. The partition function of the confined system is then given by the product of M Feynman–Wiener path integrals [14]:

$$\mathcal{Z}\left(\{\mathbf{R}_i, \mathbf{R}_i'; L_i\}\right) = \mathcal{N}\left\{\prod_{i=1}^{M}\int_{\mathbf{R}_i(0)=\mathbf{R}_i'}^{\mathbf{R}_i(L)=\mathbf{R}_i}[\mathcal{D}\mathbf{R}_i(s)]_{\text{walls}}\right\}\mathrm{e}^{-\frac{3}{2\ell}\sum_{i=1}^{M}\int_0^L\left(\frac{\partial\mathbf{R}_i(s)}{\partial s}\right)^2\mathrm{d}s} \tag{2.1}$$

$$= \mathcal{N}\int\prod_{i=1}^{M}[\mathcal{D}\mathbf{R}_i(s)]\exp\left[\sum_{i=1}^{M}\int_0^L \mathrm{d}s\left(-\frac{3}{2\ell}\dot{\mathbf{R}}_i^2(s) + A[\mathbf{R}_i(s)]\right)\right]. \tag{2.2}$$

The normalization $\mathcal{N}$ refers to the number of configurations of a collection of M completely free polymer chains, each starting at $\mathbf{R}_i'$ and ending at $\mathbf{R}_i$ in L/ℓ steps, with Kuhn steplength ℓ. In (2.2) we express the partition function as an unconfined integration by including the effect of the confining walls, which act as a constraint in the partition function (2.1), as a square well potential,

$$A[\mathbf{R}_i(s)] \equiv \ln[\Theta(\mathbf{R}_i(s)\cdot\hat{z})] + \ln[\Theta(h_z - \mathbf{R}_i(s)\cdot\hat{z})] \tag{2.3}$$

in terms of continuous arclength variables, and Θ is the unit stepfunction defined by

$$\Theta(R) = \begin{cases} 1 & \text{if} \quad R > 0 \\ 0 & \text{otherwise} \end{cases}. \tag{2.4}$$

2.1. Network formation

During network formation, the macromolecules form permanent links with one another as well as with the confining surface, resulting in the system shown in figure 1(*b*). Due to the finite size of the polymer monomers, wall links are localized a small distance $\varepsilon \sim \ell$ from the wall surface [15]. Let the set of crosslink locations—a total of N_c in the bulk and $\frac{1}{2}N_\mathrm{w}$ at each of the walls—on the chains be denoted by $\{\mathcal{S}\}$. A crosslinkage that joins points s_i^j and s_j^i on chains labelled i and j, respectively, is described mathematically by a Dirac delta constraint, $\delta\left[\mathbf{R}_i\left(s_i^j\right) - \mathbf{R}_j\left(s_j^i\right)\right]$. Similarly, the constraint $\delta[\mathbf{R}_i(s) - \boldsymbol{\eta}(x_i, y_i, \varepsilon)]$, with $\boldsymbol{\eta}$ being a three-dimensional vector determining the wall-link positions, represents a wall linkage. The set $\{\mathcal{S}\}$ of linkages is *unknown* prior to network formation, and will differ from one specimen to the next. These random crosslinks represent quenched disorder in the system. Adopting the philosophy of Deam and Edwards [8], we choose the distribution of the crosslinkages $\mathcal{P}(\{\mathcal{S}\})$ in the resultant network to be the probability of the crosslinkages an *instant* before linking. This simplified *history-dependent* situation is equivalent to a system where the future crosslinks just touch prior to an instantaneous linking.

2.2. Implementing replicas

Since the set $\{\mathcal{S}\}$ is fixed for a specific network sample, the set and its linking history will remain unaltered if the specimen is deformed in some way. Let $F(\{\mathcal{S}\})$ be the free energy of a particular sample that has been subjected to strain after network formation. The effective free energy of elasticity $\mathcal{F}(\boldsymbol{\Lambda})$ is obtained by taking the quenched average of the sample free energy over all possible realizations of the arclength locations $\{\mathcal{S}\}$,

$$\mathcal{F}(\boldsymbol{\Lambda}) = \int \mathcal{P}(\{\mathcal{S}\})F(\{\mathcal{S}\})\,\mathrm{d}\mathcal{S}_i = \int \mathcal{P}(\{\mathcal{S}\})\ln\mathcal{Z}(\{\mathcal{S}\})\,\mathrm{d}\mathcal{S}_i. \tag{2.5}$$

The averaging of the logarithm in (2.5) is facilitated by using the mathematical identity, $\lim_{n\to 0}\frac{\mathcal{Z}^n-1}{n} = \ln\mathcal{Z}$ or $\frac{\partial}{\partial n}\mathcal{Z}^n|_{n=0} = \ln\mathcal{Z}$, and replicating the system n times. For the sake

of easing the notation, we model the network by one large polymer of total length $\mathcal{L}$. Since we are interested in a resulting network with a sufficiently high crosslink density, we assume that the long chain is involved in numerous crosslinkages. The constraint—averaged over all possible positions of the links—that picks out the N_c crosslinks is given by

$$\left[\int_0^{\mathcal{L}} \mathrm{d}s \int_0^{\mathcal{L}} \mathrm{d}s' \prod_{\alpha=0}^{n} \delta[\mathbf{R}^{(\alpha)}(s) - \mathbf{R}^{(\alpha)}(s')]\right]^{N_c}. \tag{2.6}$$

The wall links are *replicated* in a similar manner. At this point, it is possible to incorporate the disorder distribution $\mathcal{P}(\{\mathcal{S}\})$, when the chains touch *before* strain, as a *zeroth* replica. The effective free energy will eventually be identified via the coefficient of n in the following generalized partition function [8]:

$$\begin{aligned}\mathcal{Z}(n) = \mathcal{N} \int [\mathcal{D}\mathbf{R}^{(0)}(s)] \widetilde{\int} \left[\prod_{\alpha=1}^{n} \mathcal{D}\mathbf{R}^{(\alpha)}(s)\right] \exp\left\{-\frac{3}{2\ell} \sum_{\alpha=0}^{n} \int_0^{\mathcal{L}} \dot{\mathbf{R}}^{(\alpha)2}\, \mathrm{d}s \right.\\ \left. + \int_0^{\mathcal{L}} A[\mathbf{R}^{(0)}(s)]\, \mathrm{d}s + \sum_{\alpha=1}^{n} \int_0^{\mathcal{L}} \tilde{A}[\mathbf{R}^{(\alpha)}(s)]\, \mathrm{d}s\right\}\\ \times \left[\int_0^{\mathcal{L}} \mathrm{d}s \int_0^{\mathcal{L}} \mathrm{d}s' \prod_{\alpha=0}^{n} \delta(\mathbf{R}^{(\alpha)}(s) - \mathbf{R}^{(\alpha)}(s'))\right]^{N_c}\\ \times \left[\int_0^{\mathcal{L}} \mathrm{d}s \int \mathrm{d}x\, \mathrm{d}y \prod_{\alpha=0}^{n} \delta(\mathbf{R}^{(\alpha)}(s) - \boldsymbol{\eta}^{(\alpha)}(x, y, \varepsilon))\right]^{N_w/2}\\ \times \left[\int_0^{\mathcal{L}} \mathrm{d}s \int \mathrm{d}x\, \mathrm{d}y \prod_{\alpha=0}^{n} \delta(\mathbf{R}^{(\alpha)}(s) - \boldsymbol{\eta}^{(\alpha)}(x, y, h_z - \varepsilon))\right]^{N_w/2}.\end{aligned} \tag{2.7}$$

Note that the crosslink points $\{\mathcal{S}\}$ are common to *all* the replicas, and so we can easily average over them. The infinitely deep, square well potential representing the wall confinement (2.3) is denoted by A in the unstrained system and by $\tilde{A}$ for the strained replicas:

$$\tilde{A}[\mathbf{R}(s)] \equiv \ln[\Theta(\mathbf{R}(s) \cdot \hat{z})] + \ln[\Theta(\lambda_z h_z - \mathbf{R}(s) \cdot \hat{z})]. \tag{2.8}$$

The integrations $\widetilde{\int}$ in (2.7) imply integration over the n deformed systems, each with volume $\widetilde{V} = \boldsymbol{\Lambda} V$, with V being the volume of the undeformed replica system and $\boldsymbol{\Lambda}$ being a deformation tensor such as (1.1).

2.3. The variational approach

Since the crosslink and confinement constraints provide a difficult path integral for the partition function, we employ the Feynman variational principle [16]. First, we introduce a new set of coordinates $\mathbf{X}^{(\beta)} \equiv \{\mathbf{X}^{(0)}, \mathbf{X}^{(1)}, \mathbf{Y}^{(m)}\}|_{\{m=1,\ldots,(n-1)\}}$, with $\mathbf{X}^{(1)}$ being a relative coordinate, and $\mathbf{X}^{(0)}$ being the centre-of-mass coordinate of all the replicas. The $n-1$ remaining coordinates are simply rotations in replica space and give the deviation of the chains from the affine position. We define the new set of coordinates in the standard way (for example see [17] and appendix A):

$$X_j^{(0)} = \frac{R_j^{(0)} + \sum_{\alpha=1}^{n} \lambda_j R_j^{(\alpha)}}{\left(1 + n\lambda_j^2\right)^{\frac{1}{2}}} \tag{2.9a}$$

$$X_j^{(1)} = \frac{\sqrt{n}\lambda_j R_j^{(0)} - \frac{1}{\sqrt{n}}\sum_{\alpha=1}^{n} R_j^{(\alpha)}}{\left(1+n\lambda_j^2\right)^{\frac{1}{2}}} \tag{2.9b}$$

$$Y_j^{(m)} = \frac{1}{\sqrt{n}}\sum_{\alpha=1}^{n} \mathrm{e}^{(2\pi \mathrm{i} m\alpha)/n} R_j^{(\alpha)} \qquad m = 1, 2, \ldots, (n-1) \tag{2.9c}$$

where the j's are Cartesian indices. These coordinates define an orthonormal transformation T with Jacobian equal to 1. The λ_j's are the elements on the diagonal of the deformation tensor $\mathbf{\Lambda}$.

The crosslink constraints are exponentiated as usual by means of chemical potentials, $B^N = \oint_{\mathbb{C}} \frac{N!}{2\pi \mathrm{i}\mu^{N+1}} \mathrm{e}^{\mu B}\,\mathrm{d}\mu$, resulting in the following compact notation:

$$\mathrm{e}^{-\mathcal{F}(\mu_\mathrm{w},\mu_\mathrm{c},n)/k_\mathrm{B}T} = \oint\oint\int \left[\prod_{\beta=0}^{n} \mathcal{D}\mathbf{X}^{(\beta)}\right] \mathrm{e}^{-\mathbb{W}+\mu_\mathrm{c}\mathbb{X}_\mathrm{c}+\mu_\mathrm{w}\mathbb{X}_\mathrm{w}+\mathbb{A}} \equiv \int [\mathrm{int}]\,\mathrm{e}^{-\mathcal{H}/k_\mathrm{B}T} \tag{2.10}$$

where $\mathcal{H}$ denotes the pseudo-Hamiltonian for network connectivity and confinement, and comprises the Wiener term,

$$\mathbb{W} \equiv -\frac{3}{2\ell}\int_0^{\mathcal{L}} \left[\dot{\mathbf{X}}^{(0)2}(s) + \dot{\mathbf{X}}^{(1)2}(s) + \sum_{m=1}^{n-1} |\dot{\mathbf{Y}}^{(m)}(s)|^2\right] \mathrm{d}s \tag{2.11}$$

the bulk crosslinks

$$\mu_\mathrm{c}\mathbb{X}_\mathrm{c} \equiv \mu_\mathrm{c}\int_0^{\mathcal{L}} \mathrm{d}s \int_0^{\mathcal{L}} \mathrm{d}s' \prod_{\beta=0}^{n} \delta\big(\mathbf{X}^{(\beta)}(s) - \mathbf{X}^{(\beta)}(s')\big) \tag{2.12}$$

the wall crosslinks

$$\begin{aligned}\mu_\mathrm{w}\mathbb{X}_\mathrm{w} \equiv \mu_\mathrm{w}\int_0^{\mathcal{L}} \mathrm{d}s \int_{-\infty}^{+\infty} \mathrm{d}x\,\mathrm{d}y \Bigg[&\delta\big(\mathbf{X}^{(0)}(s) - \boldsymbol{\nu}^{(0)}(x, y, \epsilon)\big)\delta\big(\mathbf{X}^{(1)}(s)\big)\prod_{m=1}^{n-1}\delta\big(\mathbf{Y}^{(m)}(s)\big) \\ &+ \delta\big(\mathbf{X}^{(0)}(s) - \boldsymbol{\nu}^{(0)}(x, y, h_z - \epsilon)\big)\delta\big(\mathbf{X}^{(1)}(s)\big)\prod_{m=1}^{n-1}\delta\big(\mathbf{Y}^{(m)}(s)\big)\Bigg]\end{aligned} \tag{2.13}$$

and wall constraint,

$$\mathbb{A} \equiv \int_0^{\mathcal{L}} \mathrm{d}s \left\{ A\big(T_z^{00}X_z^{(0)} + T_z^{10}X_z^{(1)}\big) + \sum_{\beta=1}^{n} \tilde{A}\big(T_z^{0\beta}X_z^{(0)} + T_z^{1\beta}X_z^{(1)} + \sum_{m=1}^{n-1} T_z^{(m+1)\beta}Y_z^{(m)}\big)\right\}. \tag{2.14}$$

We employ a harmonic trial potential to simulate the crosslink constraints

$$\mathbb{Q} = \sum_{i=x,y,z} \frac{q_i^2\ell}{6}\int_0^{\mathcal{L}} \mathrm{d}s \left[X_i^{(1)2} + \sum_{m=1}^{n-1}|Y_i^{(m)}|^2\right] \tag{2.15}$$

with q_i being the localization parameter and a measure of the limits within which each crosslink is allowed to fluctuate (if q_i is small, the crosslinking is weak). Next, we introduce a secondary trial potential, which only contains the centre-of-mass coordinate $\mathbf{X}^{(0)}$ and is defined as follows:

$$\mathbb{A}_0 \equiv \int_0^{\mathcal{L}} \mathrm{d}s \ln\left[\Theta\big(T^{00}X_z^{(0)}(s)\big)\Theta\big(h_z - T^{00}X_z^{(0)}(s)\big)\right]. \tag{2.16}$$

Using the Feynman variational principle, expression (2.10) changes to

$$\mathrm{e}^{-\mathcal{F}(\mu_{\mathrm{w}},\mu_{\mathrm{c}},n)/k_{\mathrm{B}}T} \geqslant \int \mathrm{e}^{\langle \mathbb{Q}+\mu_{\mathrm{c}}\mathbb{X}_{\mathrm{c}}+\mu_{\mathrm{w}}\mathbb{X}_{\mathrm{w}}+\mathbb{A}-\mathbb{A}_0\rangle-\mathbb{W}-\mathbb{Q}+\mathbb{A}_0} \tag{2.17a}$$

$$= \int \mathrm{e}^{\langle \mathbb{Q}+\mu_{\mathrm{c}}\mathbb{X}_{\mathrm{c}}+\mu_{\mathrm{w}}\mathbb{X}_{\mathrm{w}}+\mathbb{A}-\mathbb{A}_0\rangle} \left(\int \mathcal{G}\right) \tag{2.17b}$$

$$\equiv \mathrm{e}^{-\mathcal{F}_{\mathrm{var}}(q_x,q_z)/k_{\mathrm{B}}T} = \mathcal{Z}_{\mathrm{var}} \tag{2.17c}$$

where $\langle\cdots\rangle$ means averaging with respect to the Green's function given by

$$\int \mathcal{G} = \int [\mathcal{D}\mathbf{X}^{(0)}][\mathcal{D}\mathbf{X}^{(1)}] \left[\prod_{m=1}^{n-1} \mathcal{D}\mathbf{Y}^{(m)}\right] \underbrace{\mathrm{e}^{-\mathbb{W}-\mathbb{Q}+\mathbb{A}_0}}_{\equiv \mathrm{e}^{-\mathcal{H}_{\mathrm{var}}/k_{\mathrm{B}}T}}. \tag{2.18}$$

The resultant variational free energy is minimized with respect to the trial function, to give the best possible approximation to the real free energy $\mathcal{F}$ (for the specific choice of $\mathcal{H}_{\mathrm{var}}$), that is, $\mathcal{F} \approx \min_{\mathcal{H}_{\mathrm{var}}}\{\mathcal{F}_{\mathrm{var}}\}$. The average in the exponent in (2.17*b*) contains a *reduced* wall constraint, $\mathbb{A}-\mathbb{A}_0$, contributing terms of the order q^{-1} and smaller. In this paper, we assume a high crosslink density. This implies a large localization parameter q, so that terms of the order of q^{-1} are negligible relative to other terms, $\sim q$ and $\sim \ln q$ of (2.19)–(2.21), which play dominant roles in minimizing the free energy. The centre-of-mass coordinate $\mathbf{X}^{(0)}$ is the *only* transformed coordinate that represents physical position of the polymer chains; the $\beta > 0$ coordinates are therefore only expected to play a relatively insignificant role in localizing the network. Within the variational calculation, a *softened* wall potential $\mathbb{A}$ and high crosslink density, the averaged wall constraint becomes negligible, that is $\langle\mathbb{A}-\mathbb{A}_0\rangle \simeq 0$.

Evaluating the variational free energy $\mathcal{F}_{\mathrm{var}}(q_x, q_z)$ involves two steps. The first is calculation of the Green's functions comprising $\mathcal{G}$ (2.18). These are well-known solutions of differential equations for a random walk and are listed in appendix B. The second step is the evaluation of the weighted average $\langle\mathbb{Q}+\mu_{\mathrm{c}}\mathbb{X}_{\mathrm{c}}+\mu_{\mathrm{w}}\mathbb{X}_{\mathrm{w}}\rangle$. In the limit of total chain length larger than the spacing between the plates, $h_z \ll \sqrt{\mathcal{L}\ell}$, and a sufficiently gelled system, $\ell q_i \geqslant 1$, we obtain

$$\langle\mathbb{Q}\rangle = \frac{n}{4}\left[3+\frac{\ell\mathcal{L}}{3}(q_z+2q_x)\right] \tag{2.19}$$

$$\langle\mu_{\mathrm{w}}\mathbb{X}_{\mathrm{w}}\rangle \simeq \frac{8\mu_{\mathrm{w}}\pi^2\varepsilon^2\mathcal{L}}{h_z^3(1+n\lambda^2)^{1/2}}\left(\frac{q_z}{\pi}\right)^{n/2}\left(\frac{q_x}{\pi}\right)^{n} \tag{2.20}$$

and

$$\langle\mu_{\mathrm{c}}\mathbb{X}_{\mathrm{c}}\rangle = \frac{3\mu_{\mathrm{c}}}{2\sqrt{1+n\lambda^2}h_z}\left(\frac{q_z q_x^2}{8\pi^3}\right)^{n/2}\left[\frac{h_z\mathcal{L}^2}{V\,(1+n/\lambda)}+\frac{3\mathcal{L}}{2\pi\ell}\ln\left(\frac{\mathcal{L}}{\ell_{\mathrm{c}}}\right)\right]. \tag{2.21}$$

The chain *cut-off* length ℓ_{c}, over which the chain is not flexible but stiff, has a magnitude of the order of the Kuhn length ℓ. The variational free energy $\mathcal{F}_{\mathrm{var}}(q_x, q_z)$ of the original gel system can be identified as the coefficient of n as follows:

$$-\mathcal{F}_{\mathrm{var}}/k_{\mathrm{B}}T = \frac{\partial\mathcal{Z}_{\mathrm{var}}/\partial n|_{n=0}}{\mathcal{Z}_{\mathrm{var}}(n=0)} \tag{2.22a}$$

$$= \frac{1}{2}\frac{N_{\mathrm{c}}}{(1+c/\rho)}\left[\sum_{i=x,y,z}\lambda_i^2+\frac{c\lambda_z^2}{\rho}\right]+\frac{N_{\mathrm{w}}\lambda_z^2}{2}-\frac{\ell\pi^2\lambda_z^2\mathcal{L}}{6h_z^2}$$
$$+\frac{\ell\mathcal{L}}{12}(q_z+2q_x)-\frac{(N_{\mathrm{c}}+N_{\mathrm{w}})}{2}\sum_i\ln\left(\frac{q_i}{2\pi}\right) \tag{2.22b}$$

where

$$c = \frac{3}{2\pi \ell h_z} \ln \frac{\mathcal{L}}{\ell_c} \quad \text{and} \quad \rho = \mathcal{L}/V. \tag{2.23}$$

Next the free energy is minimized with respect to q_x and q_z to find the best approximation to the real free energy of the system. The resultant stationary points are isotropic and deformation independent:

$$q_x = \frac{6(N_w + N_c)}{\ell \mathcal{L}} = q_z. \tag{2.24}$$

Substituting the q-values into (2.22*b*), we find that the free energy on deformation has the following upper bound (showing only the λ-dependent terms):

$$\mathcal{F}(\mathbf{\Lambda}) \leqslant k_B T \left\{ \frac{1}{2} \frac{N_c}{(1 + c/\rho)} \left[\sum_{i=x,y,z} \lambda_i^2 + \frac{c\lambda_z^2}{\rho} \right] + \frac{N_w \lambda_z^2}{2} - \frac{\ell \pi^2 \lambda_z^2 \mathcal{L}}{6h_z^2} \right\}. \tag{2.25}$$

2.4. The stress–strain relationship

The stress f, which is the elastic force per unit area of the undeformed cross-section of the sample, in the specific case of a uniaxial isovolumetric deformation (1.1), is given by

$$f = \frac{1}{V} \frac{\partial \mathcal{F}}{\partial \lambda} = \frac{k_B T}{V} \left[\frac{N_c}{(1 + c/\rho)} \left\{ \underline{\lambda - \frac{1}{\lambda^2}} + \frac{c}{\rho} \lambda \right\} + \left(N_w - \frac{\pi^2 \ell \mathcal{L}}{3h_z^2} \right) \lambda \right]. \tag{2.26}$$

The underlined part in (2.26) coincides with the well-known result of the classical theory of high elasticity of polymer networks [7], apart from the different front factor $g \equiv (1 + c/\rho)^{-1}$, which may be attributed to wasted loops [8].

The wall confinement introduces new terms in the free energy of the network, dependent on the spacing h_z between the walls. For example, the typical confinement term $\sim k_B T \frac{\ell \mathcal{L}}{h_z^2}$ is consistent with earlier results for simpler networks [19] and a single chain with an effective contourlength $\mathcal{L}$ [20, 21].

Unfortunately, the model employed in this section is too crude to differentiate between the types of crosslinking. This resulted in the wall links and bulk links being treated in the same manner. Intuitively, the degree of localization, manifested in the values q_x and q_z, is expected to depend on the spatial coordinate. In the next section a polymer brush network is investigated. Within this framework, it is possible to distinguish, in a simple albeit concise manner, between the localization that each type of crosslink imposes.

3. The brush network

In this section we consider the network in figure 2(*b*) formed from two grafted polymer brushes. The term *polymer brush* was invented by de Gennes [22] to describe an architecture in which polymer chains are terminally tethered to a surface at a high density. The best way to realize a brush network is to grow chains directly at the surface of the wall. This approach is called *grafting* and is shown in figure 2(*a*). Firstly the surface is covered with a monolayer of *initiator* molecules, from which long molecules grow like a lawn[1]. Secondly, the brush chains are sufficiently crosslinked. Each *brush* consists of $\frac{1}{2}N_w$ ideal chains that are

[1] We assume, as in the previous section, that the polymer chains are linked an infinitesimal distance ε away from the wall surface. In this case, the ε can be interpreted as the *size* of the initiator molecules, from which the chains are grafted.

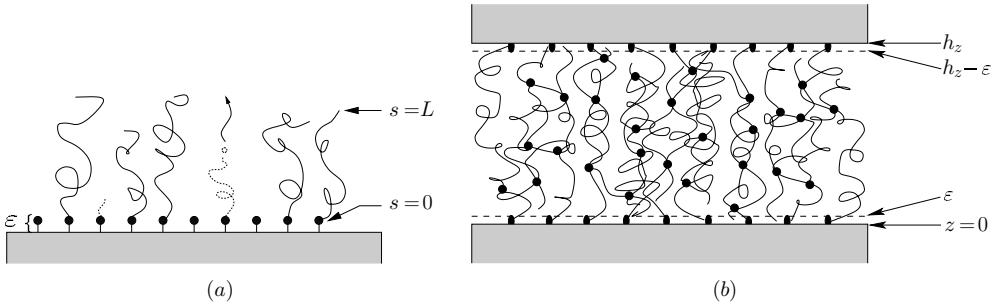

Figure 2. (*a*) A schematic illustration of polymer chains grafting from a solid surface, a brush, consisting of polymer chains permanently attached to a flat, solid surface. (*b*) A brush network.

permanently attached via endpoints to the confining surface. Each *chain* has contourlength L and participates in N_c crosslinkages. The formation of a brush network differs from the melt network in section 2, since surface attachment and crosslinking are not performed simultaneously, but in subsequent steps.

3.1. Trial potential for the brush network

The anticipated behaviour (within the replica scheme) of a surface-attached, crosslinked polymer includes some kind of localization of the polymer. In section 2 we employed the idea of Deam and Edwards [8], which treats this localization to be homogeneous and translation invariant, that is $q_x = q_z =$ constant in the trial potential $\mathbb{Q}$ given by (2.15). We expect the polymer to be localized differently near the surface than in the bulk region away from the surfaces. This implies that the variational parameters q_i should depend on the spatial height $z(s)$, of a polymer segment s, between the plates. The only coordinate in the transformed replica system (2.9*a*), which represents physical position of the chain segments, is the 'centre-of-mass' coordinate $\mathbf{X}^{(0)}$. Mathematically, it is thus possible to distinguish between different localizations, by using a trial potential of the form

$$\mathbb{Q} \sim \int \mathrm{d}s\, q^2\,(z(s)) \sum_{\beta=1}^{n} \mathbf{X}^{(\beta)2} \tag{3.1}$$

with the localization parameter q being a function of $z(s) \equiv \hat{z} \cdot \mathbf{X}^{(0)}(s)$. Unfortunately, the path integration of a harmonic potential, which is dependent on the arclength coordinate s and a mixture of configurational coordinates of *different* replicas, seems intractable. However, in a brush network each stretched-out chain is only attached by one *endpoint* ($s = 0$) to the grafting surface, as shown in figure 2(*a*). Consequently, we choose the average localization to be solely dependent on s, and not the spatial position of the chain. It is now possible to simulate the crosslink constraints by the following trial harmonic potential (compare with (2.15)),

$$\mathbb{Q} = \frac{1}{6\ell} \sum_{\beta=1}^{n} \left(\int_0^{\tau} \mathrm{d}s\, q_0^2 \mathbf{X}^{(\beta)2} + \int_{\tau}^{L} \mathrm{d}s\, q_1^2 \mathbf{X}^{(\beta)2} \right) \tag{3.2}$$

and thus model the system variationally by means of *three* variational parameters q_0, q_1 and τ, shown in figure 3.

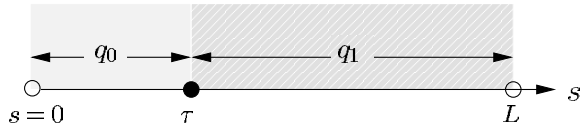

Figure 3. The s-line depicts the domains of the variational parameters, q_0, q_1 and τ in (3.2).

3.2. The brush network free energy

The variational calculation for the brush network corresponds to the previous calculation in section 2.3, except for the new trial potential $\mathbb{Q}$ defined in (3.2). In order to simplify the minimization task, we choose $q_0 = (1+\gamma)q_1$, with γ being a real number. Referring to the average $\langle \mathbb{Q} + \mu_c \mathbb{X}_c + \mu_w \mathbb{X}_w \rangle$ calculated in appendix C, the variational free energy in $3(n+1)$ replica space is given by

$$\mathcal{Z}_{\text{var}}(n, q_1, \gamma, \tau) = \prod_{i=1}^{N_w} \mathrm{e}^{\langle \mu_c \mathbb{X}_c + \mu_w \mathbb{X}_w + \mathbb{Q} \rangle} \left(\int \mathcal{G} \right) \tag{3.3a}$$

$$= \prod_{i=1}^{N_w} \langle \mathbb{X}_c \rangle^{N_c} \langle \mathbb{X}_w \rangle^{N_w} \mathrm{e}^{\frac{nq_1\ell}{4}(\gamma\tau + L)} \left(\int \mathcal{G} \right). \tag{3.3b}$$

The variational free energy of the original three-dimensional brush network is obtained from the limiting procedure (2.22*a*),

$$\begin{aligned}
\mathcal{F}_{\text{var}}(q_1, \gamma, \tau)/k_B T = {} & \frac{\ell N_w}{4} (L + \gamma\tau)\, q_1 - \frac{\ell L \lambda^2 N_w \pi^2}{6 h_z^2} - \frac{3}{2} N_w \ln\left(\frac{4(1+\gamma)}{2+\gamma} \right) \\
& - \frac{3}{2} N_c N_w \ln\left(\frac{q_1}{2\pi} \right) - N_c N_w \left[\frac{3}{2} \ln(1+\gamma) \left\{ \frac{3}{\pi \ell h_z} \left(\ell_c - \sqrt{\ell_c^2 + \tau^2} \right. \right. \right. \\
& \left. \left. \left. + \frac{\tau}{2} \ln\left[\frac{\sqrt{\ell_c^2 + \tau^2} + \tau}{\sqrt{\ell_c^2 + \tau^2} - \tau} \right] \right) + \frac{2 N_w \tau^2}{V} \right\} + \frac{3}{2} \ln\left[\frac{2(1+\gamma)}{2+\gamma} \right] \left\{ \frac{4 N_w (L-\tau)\tau}{V} \right. \\
& - \frac{3}{\pi \ell h_z} \left(\ell_c + \sqrt{\ell_c^2 + L^2} - \sqrt{\ell_c^2 + (L-\tau)^2} - \sqrt{\ell_c^2 + \tau^2} \right. \\
& \left. \left. - L \ln\left[\frac{\sqrt{\ell_c^2 + (L-\tau)^2} - L + \tau}{\sqrt{\ell_c^2 + L^2} - L} \right] - \tau \ln\left[\frac{\sqrt{\ell_c^2 + \tau^2} - \tau}{\sqrt{\ell_c^2 + (L-\tau)^2} - L + \tau} \right] \right) \right\} \\
& \left. - \frac{N_w L^2}{V} \sum_{i=x,y,z} \lambda_i^2 - \frac{3\lambda_z^2}{2\pi \ell h_z} \left(\ell_c - \sqrt{\ell_c^2 + L^2} + \frac{L}{2} \ln\left[\frac{\sqrt{\ell_c^2 + L^2} + L}{\sqrt{\ell_c^2 + L^2} - L} \right] \right) \right] \\
& \times \left(\frac{2 N_w L^2}{V} + \frac{3}{\pi \ell h_z} \left(\ell_c - \sqrt{\ell_c^2 + L^2} + \frac{L}{2} \ln\left[\frac{\sqrt{\ell_c^2 + L^2} + L}{\sqrt{\ell_c^2 + L^2} - L} \right] \right) \right)^{-1}.
\end{aligned} \tag{3.4}$$

Finding the stationary points $\{q_1^*, \gamma^*, \tau^*\}$, where $\mathcal{F}_{\text{var}}$ has a global minimum, is formidable and calls for a numerical calculation. However, it is possible to obtain q_1^* and γ^* (and thus also q_0^*) analytically where γ^* is still a function of τ:

$$q_1^* = \frac{6 N_c}{\ell (L + \gamma^*)} \qquad \text{and} \qquad q_0^* = \frac{6 N_c (1+\gamma^*)}{\ell (L + \gamma^*)}. \tag{3.5}$$

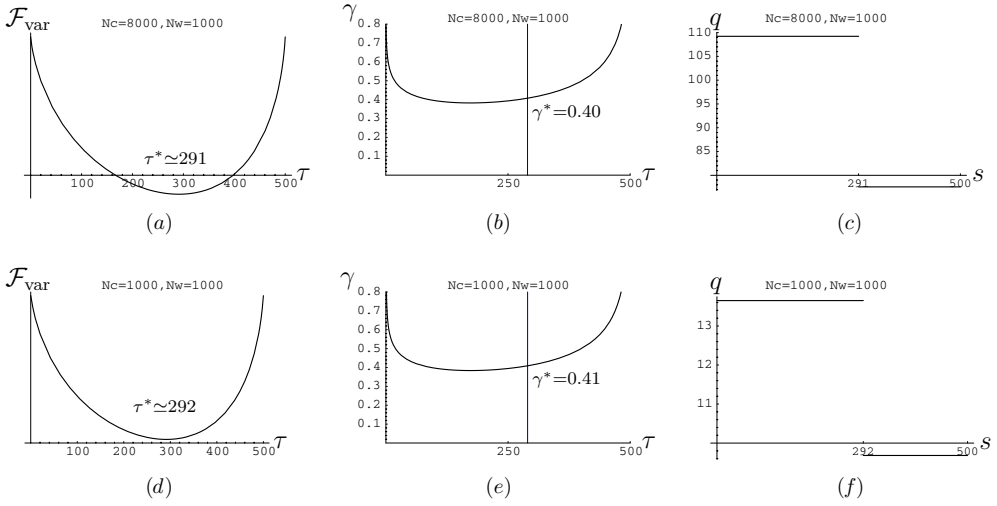

Figure 4. Investigating the influence of the crosslink density $N_{\rm c}$ on the localization of the polymer. The leftmost column of graphs depicts the variational free energy as a function of τ. The rightmost column illustrates that $q_0 > q_1$. Plots were rendered with the following kept constant: $L = 500$, $h_z = 20, \lambda = 1, \ell = \ell_{\rm c} = 1, \rho = 0.4$.

The value τ^*, which minimizes the free energy $\mathcal{F}_{\rm var}$, is found by plotting the free energy as a function of τ, and identifying τ^* as the value, on region $(\ell_{\rm c}, L - \ell_{\rm c})$, where $\mathcal{F}_{\rm var}(\tau)$ has a global minimum.

3.3. The homogeneous brush limit

In a homogeneous brush network, the crosslinks impose a uniform localization on the system. This situation is obtained by letting $\tau = 0$ or $\gamma = 0$ in (3.5) and (3.4) respectively. In this limit we obtain the usual Deam and Edwards [8] localization parameters, $q_1^* = \frac{6N_{\rm c}}{\ell L} = q_0^*$, and the following free energy of deformation

$$\mathcal{F}_{\rm hom} \geqslant k_{\rm B}T \left\{ \frac{1}{2}\frac{N_{\rm c}N_{\rm w}}{(1+c/\rho)}\Big[\sum_{i=x,y,z} \lambda_i^2 + \frac{c}{\rho}\lambda_z^2 \Big] - \frac{\pi^2 \ell L \lambda_z^2 N_{\rm w}}{6h_z^2} + \begin{matrix}\lambda\text{-independent} \\ \text{terms}\end{matrix} \right\} \tag{3.6}$$

with

$$\rho = \frac{N_{\rm w}L}{V} \quad \text{and} \quad c \equiv \frac{3}{2\pi \ell h_z L}\left(\ell_{\rm c} - \sqrt{\ell_{\rm c}^2 + L^2} + \frac{L}{2}\ln\left[\frac{\sqrt{\ell_{\rm c}^2 + L^2} + L}{\sqrt{\ell_{\rm c}^2 + L^2} - L} \right] \right) \tag{3.7}$$

which closely resembles the free energy (2.25) of the melt network[2], apart from a different c-value (2.23).

3.4. Localization of the polymer brush network

Next, we examine the graphs in figure 4 to see how the linking density $N_{\rm c}$ influences the localization of the polymer. Each row in figure 4 corresponds to a different value of $N_{\rm c}$. The

[2] Here, the total number of crosslinks in the sample is given by $N_{\rm c}N_{\rm w}$.

first observation that can be made is that the chains in the 'surface' region (q_0) are localized to a greater extent than the chains away from the walls (q_1). This follows from the fact that γ^* is positive in the middle column of figure 4, and so we have that $q_1 < q_0$ from (3.5). The measure of the fluctuations of the crosslinks from their affine positions, given by the q-values, is greater for a chain that is lightly crosslinked as shown in figure 4, than for a network where $N_c > N_w$. Since $\gamma^* < 1$, the q-values (3.5) are primarily influenced by the number of crosslinks $N_c N_w$.

3.5. Elasticity

A closed form for the stress–strain relationship is attainable, since the variational parameters q_0, q_1 and τ do not depend on the affine deformation of the system. By differentiating the variational free energy in (3.4) with respect to λ, one obtains the following stress–strain relationship:

$$f(\lambda) = \frac{k_B T}{V}\left[\frac{N_c N_w}{(1+c/\rho)}\left\{\underline{\lambda - 1/\lambda^2} + \frac{c}{\rho}\lambda\right\} - \frac{\pi^2 \ell L N_w}{3h_z^2}\lambda\right] \tag{3.8}$$

where the polymer density ρ and the factor c are defined in (3.7). This result is consistent with the stress–strain relationship for the melt network apart from different c-values and by letting $\mathcal{L} = LN_w$. In the melt network, both wall links and bulk links are formed simultaneously and have the freedom to form anywhere along the length of the polymer chains, in contrast with a brush network. This difference is portrayed in the $N_w\lambda$ term in (2.26), which is absent from the brush network stress–strain equation.

4. Conclusion

In this paper we investigated the elastic properties of two different confined, surface-attached network models. The distance h_z between the confining walls was chosen to be smaller than the effective size $\sqrt{\mathcal{L}\ell}$ of the network. Calculations were presented for a sufficiently high crosslink density—a high localization regime—not a system in the vicinity of the sol-gel transition point [25].

The melt network of section 2 was formed from pre-existing, confined macromolecules, that were crosslinked *simultaneously* to each other and to the confining surface. Since we employed a harmonic potential identical to that of Deam and Edwards, with isotropic, homogeneous localization, we found the localization parameters to be equal, $q_x = q_z$, and analogous to that of an unconfined network model. They were namely strain independent, and proportional to the mean square radius of gyration of a chain piece between two junction points. In terms of localization, the wall links were treated as bulk links, $q = \frac{6(N_c+N_w)}{\ell\mathcal{L}}$, where $\mathcal{L}$ is the effective contourlength of the giant network polymer, ℓ is the Kuhn steplength, and N_c and N_w are the total number of bulk links and wall links, respectively. The quantity $q^{-1/2}$ gives a measure of the fluctuation of the network chains from the mean affine deformation path. In other words, it defines the relative diameter of a tube in which each chain is confined due to the surrounding crosslink constraints.

Next, we investigated a surface-attached network, fabricated via an instantaneous crosslinking of two pre-existing polymer brushes. This architecture was specifically chosen to facilitate an *inhomogeneous* localization scheme. The effect of the crosslink and wall constraints was modelled by two constant localization parameters q_0 and q_1, which were arclength dependent. We found each chain to be localized to a greater degree near the surface at which it is attached, than far away from its grafting surface ($q_0 > q_1$). The great advantage

Table 1. The g-factors give an estimate of the percentage fraction of crosslinks that are elastically active. Estimates are for a network fabricated from $N_w = 1000$ chains of chain length $L = 500$, polymer density $\rho = 0.4$, chain cut-off length $\ell_c = 1 = \ell$ and confinement $h_z = 20$, where lengths are in units of ℓ.

	Unconfined	Confined	
	Deam Edwards	Melt network	Brush network
c	0.17	0.31	0.14
g	0.70	0.56	0.74

of this scheme is the fact that the wall links were not treated as bulk links, but played a role in the arc length distance over which each constant localization takes effect.

Common to both the brush network and the melt network was the general form (apart from constants) of the stress–strain relationship $f(\lambda)$ for a uniaxial, isovolumetric deformation (recall expressions (2.26) and (3.8)). The underlined part in both these expressions gives the characteristic curve of classic rubber elasticity models, with the slope characterized by a *different* elastic modulus than encountered in the usual unconfined models. There are two new additions to the result of Deam and Edwards for a model with unconfined, ideal chains. The first is the c/ρ term, due to wall links and the second, h_z-dependent term, is due to the confinement. Stress–strain measurements in uniaxial extension should therefore be able to distinguish between wall-link histories and the role of the parameter h_z for suitably prepared systems. To the authors' knowledge, no such experiments on confined systems have yet been performed. The front factor $g \equiv (1 + c/\rho)^{-1}$, also encountered in the Deam and Edwards result (1.3), gives a measure of the number of elastically active crosslinks in the system (see table 1).

An obvious improvement of the present phantom (i.e. ideal chain) models should include trapped entanglements and excluded volume effects. This could for example be based on a non-Gaussian tube model or slip-link model [26] with non-affine deformation. These improvements would make it possible to compare theoretical results with simulations (see e.g. [27]), which generally tend to focus on topological issues.

The variational calculation is extremely difficult when the localization potential depends on the relevant spatial position, say $z(s)$, between the parallel plates. For this reason, we chose a simple arclength dependence. However, it might still be possible to find a potential that is tractable and more representative of the surface-confinement problem.

Acknowledgments

Financial assistance from the Department of Labour (DoL), National Research Foundation of South Africa and Stellenbosch University is hereby acknowledged.

Appendix A. Coordinate transformation

The coordinates $X_j^{(\beta)}(s) = T_j^{\beta\alpha} R_j^{(\alpha)}(s)$ define an orthogonal transformation with Jacobian equal to 1. Cartesian coordinates x, y, z are represented by j. The index m runs from 1 to $n - 1$; therefore, $m = 1 \Leftrightarrow \beta = 2$. In matrix form the transformation T may look as follows:

$$\mathsf{T}_j = \begin{pmatrix} \left(1+n\lambda_j^2\right)^{-\frac{1}{2}} & \lambda_j\left(1+n\lambda_j^2\right)^{-\frac{1}{2}} & \lambda_j\left(1+n\lambda_j^2\right)^{-\frac{1}{2}} & \dots \\ \sqrt{n}\lambda_j\left(1+n\lambda_j^2\right)^{-\frac{1}{2}} & -\frac{1}{\sqrt{n}}\left(1+n\lambda_j^2\right)^{-\frac{1}{2}} & -\frac{1}{\sqrt{n}}\left(1+n\lambda_j^2\right)^{-\frac{1}{2}} & \dots \\ 0 & \frac{1}{\sqrt{n}}\,\mathrm{e}^{(2\pi \mathrm{i} m\alpha)/n} & \frac{1}{\sqrt{n}}\,\mathrm{e}^{(2\pi \mathrm{i} m\alpha)/n} & \dots \\ \vdots & \vdots & \vdots & \ddots \end{pmatrix}. \tag{A.1}$$

This is the most symmetric transformation method [8], but there also exist other transformations, notably in [23], where all entries are chosen to be real. The factor $\left(1+n\lambda_j^2\right)^{1/2}$ ensures the orthonormality of the transformation.

The wall-crosslink position vectors $\eta^{(\alpha)}$ are transformed in the same way as the polymer chain coordinates $\mathbf{R}^{(\alpha)}$ by the transformation T (A.1) as follows: $\nu_j^{(0)}(s) = T_j^{0\alpha}\eta_j^{(\alpha)}(s)$, $\nu_j^{(1)}(s) = T_j^{1\alpha}\eta_j^{(\alpha)}(s)$ and $\omega_j^{(m)}(s) = T_j^{m\alpha}\eta_j^{(\alpha)}(s)$.

Appendix B. The Green's functions

The following path integrals are well-known solutions to differential equations [16, 24] describing a free random walk

$$\begin{aligned}\mathcal{G}_0\left(X_{is}^{(0)}, X_{is'}^{(0)}, |s-s'|\right) &= \mathcal{N}\int \left[\mathcal{D}X_i^{(0)}\right] \mathrm{e}^{-\frac{3}{2\ell}\int_0^{\mathcal{L}} \dot{X}_i^{(0)2}\mathrm{d}s} \qquad [\text{for} \quad i=\{x,y\}] \\ &= \frac{1}{V_i(1+n\lambda^2)^{\frac{1}{2}}} + \left(\frac{3}{2\pi\ell|s-s'|}\right)^{\frac{1}{2}} \exp\left\{-\frac{3}{2\ell}\frac{\left(X_{is}^{(0)}-X_{is'}^{(0)}\right)^2}{|s-s'|}\right\}\end{aligned} \tag{B.1}$$

a random walk confined between two planar surfaces,

$$\begin{aligned}\mathcal{G}_0\left(X_{zs}^{(0)}, X_{zs'}^{(0)}, |s-s'|\right) &= \mathcal{N}\int \left[\mathcal{D}X_z^{(0)}\right] \exp\left\{-\frac{3}{2\ell}\int_0^{\mathcal{L}} \dot{X}_z^{(0)2}\,\mathrm{d}s \right. \\ &\qquad \left. + \int_0^{\mathcal{L}} \ln\left[\Theta\left(T^{00}X_z^{(0)}\right)\Theta\left(h_z - T^{00}X_z^{(0)}\right)\right]\mathrm{d}s\right\} \\ &= \frac{2}{\sqrt{1+n\lambda^2}h_z}\sum_{p=1}^{\infty} \mathrm{e}^{-\frac{\ell\pi^2p^2}{6h_z^2}|s-s'|} \sin\left[\frac{\pi p X_z^{(0)}(s)}{\sqrt{1+n\lambda^2}h_z}\right]\sin\left[\frac{\pi p X_z^{(0)}(s')}{\sqrt{1+n\lambda^2}h_z}\right]\end{aligned} \tag{B.2}$$

and a random walk in a harmonic potential (for replicas $\beta > 0$)

$$\begin{aligned}\mathcal{G}_\beta\left(\mathbf{X}_s^{(\beta)}, \mathbf{X}_{s'}^{(\beta)}, |s-s'|\right) &= \mathcal{N}\int \left[\mathcal{D}\mathbf{X}^{(\beta)}\right] \mathrm{e}^{-\frac{3}{2\ell}\int_0^{\mathcal{L}} \dot{\mathbf{X}}^{(\beta)2}\,\mathrm{d}s - \frac{q_i^2 l}{6}\int_0^{\mathcal{L}} \mathbf{X}^{(\beta)2}\,\mathrm{d}s} \\ &= \left(\frac{q_i}{2\pi\,\sinh\frac{1}{3}\ell q_i|s-s'|}\right)^{\frac{1}{2}} \mathrm{e}^{-\frac{q_i}{2}\frac{(\mathbf{X}^{(\beta)2}(s)+\mathbf{X}^{(\beta)2}(s'))\cosh\frac{1}{3}\ell q_i|s-s'| - 2\mathbf{X}^{(\beta)}(s)\mathbf{X}^{(\beta)}(s')}{\sinh\frac{1}{3}\ell q_i|s-s'|}}.\end{aligned} \tag{B.3}$$

In this paper we investigate the limit $\sqrt{\mathcal{L}\ell} \gg h_z$ and accordingly only the first term ($p = 1$) in the sum of (B.2) is considered important (see also p 20 of [13]). Furthermore, for a sufficiently strong localization q, only the lowest eigenfunction significantly contributes to $\mathcal{G}$ and it is acceptable [8] to approximate (B.3) by

$$\mathcal{G}_\beta\left(X_s^{(\beta)}, X_{s'}^{(\beta)}, |s-s'|\right) \simeq \left(\frac{q_i}{\pi}\right)^{\frac{1}{2}} \exp\left\{-\frac{q_i}{2}\left(X_s^{(\beta)2} + X_{s'}^{(\beta)2} + \frac{\ell}{3}|s-s'|\right)\right\} \tag{B.4}$$

such that (B.4) is used to perform the $\beta > 0$ bulk-link averages (2.12).

Appendix C. Brush averages

The weighted average of the bulk-link contribution in (3.3*a*), with $i = 1, 2, \ldots, N_{\mathrm{w}}$, is

$$\langle \mu_{\mathrm{c}} \mathbb{X}_{\mathrm{c}} \rangle = \left\langle \mu_{\mathrm{c}} \sum_{j=1}^{N_{\mathrm{w}}} \int_0^{\mathcal{L}} \mathrm{d}s \int_0^{\mathcal{L}} \mathrm{d}s' \prod_{\beta=0}^{n} \delta\big(\mathbf{X}_i^{(\beta)}(s) - \mathbf{X}_j^{(\beta)}(s')\big) \right\rangle \tag{C.1}$$

$$\begin{aligned} &= \frac{3\mu_{\mathrm{c}}}{2h_z\sqrt{1+n\lambda^2}} \int_0^{\tau} \mathrm{d}s \int_0^{\tau} \mathrm{d}s' \left(\frac{2N_{\mathrm{w}}h_z}{V(1+n/\lambda)} + \frac{3}{2\pi\ell|s-s'|} \right) \left(\frac{q_0}{2\pi} \right)^{\frac{3n}{2}} \\ &\quad + 2\int_0^{\tau} \mathrm{d}s \int_{\tau}^{L} \mathrm{d}s' \left(\frac{2N_{\mathrm{w}}h_z}{V(1+n/\lambda)} + \frac{3}{2\pi\ell|s-s'|} \right) \left(\frac{q_0 q_1}{\pi(q_0+q_1)} \right)^{\frac{3n}{2}} \\ &\quad + \int_{\tau}^{L} \mathrm{d}s \int_{\tau}^{L} \mathrm{d}s' \left(\frac{2N_{\mathrm{w}}h_z}{V(1+n/\lambda)} + \frac{3}{2\pi\ell|s-s'|} \right) \left(\frac{q_1}{2\pi} \right)^{\frac{3n}{2}}. \end{aligned} \tag{C.2}$$

The Gaussian chain model and continuous chain coordinates s are only valid when we look at length scales larger than a certain length, say ℓ_{c}. When $s < \ell_{\mathrm{c}}$, the molecule is no longer a flexible, continuous chain: it consists of monomers with rigid bonds. Therefore, we make the substitution: $|s-s'|^{-1} \longrightarrow \lim_{\ell_{\mathrm{c}}\to 0} \left[(s-s')^2 + \ell_{\mathrm{c}}^2\right]^{-1/2}$, which leads to a straightforward integration and the result shown in (3.4).

The wall links in the brush network only occur at $s = 0$. Consequently, the average $\langle \mu_{\mathrm{w}} \mathbb{X}_{\mathrm{w}} \rangle$ for the melt network is adapted to suit the brush network average (2.13) by the substitution $\mathbb{X}_{\mathrm{w}}|_{s=0}$ and the absence of the s integration. This leads to

$$\langle \mu_{\mathrm{w}} \mathbb{X}_{\mathrm{w}} \rangle = \frac{4\mu_{\mathrm{w}}\pi^2\varepsilon^2}{h_z^3}. \tag{C.3}$$

The average of the harmonic trial potential for inhomogeneous localization is given by the following expression:

$$\langle \mathbb{Q} \rangle = \left\langle \frac{\ell q_0^2}{6} \int_0^{\tau} \mathrm{d}s \left(\mathbf{X}_i^{(1)2} + \sum_{m=1}^{n-1} \left|\mathbf{Y}_i^{(m)}\right|^2 \right) + \frac{\ell q_1^2}{6} \int_{\tau}^{L} \mathrm{d}s \left(\mathbf{X}_i^{(1)2} + \sum_{m=1}^{n-1} \left|\mathbf{Y}_i^{(m)}\right|^2 \right) \right\rangle \tag{C.4}$$

$$\simeq \frac{n\ell}{4} \left[(q_0 - q_1)\,\tau + q_1 L \right] \qquad \text{when} \quad q_0 \geqslant \frac{3}{\ell\tau} \quad \text{and} \quad q_1 \geqslant \frac{3}{\ell(L-\tau)}. \tag{C.5}$$

References

[1] Paul S 1986 *Surface Coatings: Science and Technology* 2nd edn (New York: Wiley)
[2] Ratner B D 1989 Biomedical applications of synthetic polymers *The Synthesis, Characterization, Reactions and Applications of Polymers* vol 7 (New York: Pergamon)
[3] See for example,Vilgis T A 2000 *Phy. Rep*. **336** 167, and references therein
[4] Allegra G and Raos G 2002 *J. Chem. Phys*. **116** 3109
[5] Treloar L R G 1958 *The Physics of Rubber Elasticity* 2nd edn (Oxford: Clarendon)
[6] Kuhn W 1934 *Kolloid Z*. **68** 2
[7] James H M and Guth E 1943 *J. Chem. Phys*. **11** 455
[8] Deam R T and Edwards S F 1976 *Proc. R. Soc*. A **280** 317
[9] Edwards S F and Anderson P W 1975 *J. Phys. F: Met. Phys*. **5** 965
[10] Panyukov S and Rabin Y 1996 *Phy. Rep*. **269** 1
[11] Young R J and Lovell P A 1991 *Introduction to Polymers* (Cheltenham: Stanley Thornes)
[12] Prucker O, Müller K and Rühe J 2000 *Interfaces, Adhesion and Processing in Polymer Systems* vol 629, ed G S Ferguson, S H Anastasiadis and A Karim (Warrendale: Materials Research Society)

[13] Edwards S F and Doi M 1986 *The Theory of Polymer Dynamics* (Oxford: Clarendon)
[14] Freed K F and Edwards S F 1969 *J. Phys. A: Gen. Phys.* **2** 145
[15] The factor ε does not contribute to the deformation free energy. Also see Dolan A K and Edwards S F 1973 *Proc. R. Soc.* A **337** p 511
[16] Feynman R P and Hibbs A R 1965 *Quantum Mechanics and Path Integrals* (New York: McGraw-Hill)
[17] Edwards S F 1972 *Polymer Networks* ed A J Chompff *et al* (New York: Plenum)
[18] Ball R C and Edwards S F 1980 *Macromolecules* **13** 748
[19] Vandoolaeghe W L 2003 Polymer networks at surfaces *Master's Thesis,* Stellenbosch University
[20] De Gennes P G 1985 *Scaling Concepts in Polymer Physics* (Ithaca: Cornell University Press) p 34
[21] Grosberg A Y and Khoklov A R 1994 *Statistical Physics of Macromolecules* (New York: AIP) p 42
[22] De Gennes P G 1980 *Macromolecules* **13** 1069
[23] Ball R C, Edwards S F, Doi M and Warner M 1981 *Polymer* **22** 1010
[24] Wiegel F W 1986 *Introduction to Path Integral Methods in Physics and Polymer Science* 1st edn (Singapore: World Scientific)
[25] Theoretical treatments of the gel-point transition still remain difficult. For example see Goldbart P and Goldenfeld N 1989 *Phys. Rev.* A **39** 1402
[26] Vilgis T A and Edwards S F 1988 *Rep. Prog. Phys.* **51** 243
[27] Everaers R and Kremer K 1996 *Phys. Rev.* E **53** 1